

Integrating Display and Delivery Functionality with a Cell Penetrating Peptide Mimic as a Scaffold for Intracellular Multivalent Multitargeting

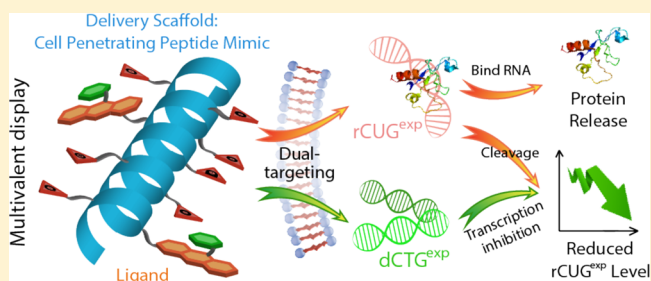
Yugang Bai,^{†,||} Lien Nguyen,^{†,||} Ziyuan Song,^{‡,||} Shaohong Peng,[§] JuYeon Lee,[†] Nan Zheng,[‡] Iti Kapoor,[†] Lauren D. Hagler,[†] Kaimin Cai,[‡] Jianjun Cheng,[‡] H. Y. Edwin Chan,[§] and Steven C. Zimmerman^{*,†}

[†]Department of Chemistry and [‡]Department of Materials Science and Engineering, University of Illinois at Urbana–Champaign, Urbana, Illinois 61801, United States

[§]Laboratory of Drosophila Research and School of Life Sciences, The Chinese University of Hong Kong, Shatin, New Territories, Hong Kong SAR, China

S Supporting Information

ABSTRACT: The construction of a multivalent ligand is an effective way to increase affinity and selectivity toward biomolecular targets with multiple-ligand binding sites. Adopting this strategy, we used a known cell-penetrating peptide (CPP) mimic as a scaffold to develop a series of multivalent ligand constructs that bind to the expanded dCTG (CTG^{exp}) and rCUG nucleotide repeats (CUG^{exp}) known to cause myotonic dystrophy type I (DM1), an incurable neuromuscular disease. By assembling this polyvalent construct, the hydrophobic ligands are solubilized and delivered into cell nuclei, and their enhanced binding affinity leads to the inhibition of ribonuclear foci formation and a reversal of splicing defects, all at low concentrations. Some of the multivalent ligands are shown to inhibit selectively the *in vitro* transcription of (CTG·CAG)₇₄ to reduce the concentration of the toxic CUG RNA in DM1 model cells, and to show phenotypic improvement *in vivo* in a *Drosophila* model of DM1. This strategy may be useful in drug design for other trinucleotide repeat disorders and more broadly for intracellular multivalent targeting.



INTRODUCTION

Oligovalent or polyvalent (multivalent) ligands are synthetic constructs that present multiple copies of receptor-binding moieties. Compared with their monovalent analogs, these constructs offer both thermodynamic and kinetic advantages originating from a range of mechanisms including the chelate effect, subsite binding, steric stabilization, receptor clustering, and statistical and local concentration effects.¹ Not surprisingly, the affinity of multivalent ligands toward their biological targets is highly dependent on the molecular structure and conformation of ligands in aqueous solution. Well-designed multivalent constructs may afford significant enhancements in affinity and selectivity toward their targets.² Indeed, the use of multivalency is now an established, effective strategy for developing potent inhibitors of a range of biological processes.³

The majority of reported multivalent ligands function at the cell surface. Although multivalent ligands for intracellular targets have been reported,⁴ an obvious limitation is the need for large structures to pass the cell membrane. Polyvalent constructs have been developed as targeted delivery vehicles,⁵ some of which enter the cell by endocytosis and deliver their cargo.⁶ Such approaches are especially important for cancer therapy allowing significant quantities of hydrophobic cytotoxic agents to be delivered selectively to cells within the target

tissue.^{2f,g,5} By encapsulating large quantities of the drug in a nanoscale vehicle that enhances selective localization through the display of multiple copies of a targeting moiety, the polyvalent construct becomes an essential part of the therapeutic formulation, increasing local drug concentration and reducing unwanted, off-site cytotoxicity.

An important class of intracellular therapeutic targets, well suited to a multivalent ligand approach, is found in a set of rare diseases, known as trinucleotide repeat expansion diseases (TREDs). TREDs are associated with unstable microsatellites, for example, Huntington's disease, myotonic dystrophy type 1 (DM1), fragile X syndrome, and various spinocerebellar ataxias being associated with CAG^{exp}, CTG^{exp}, CCG^{exp}, and CNG^{exp} repeats, respectively.⁷ In the case of DM1, the CTG expansion located in the 3'-untranslated region of the dystrophin myotonia protein kinase (*DMPK*) gene produces a toxic CUG^{exp} transcript. Thus, as outlined in Figure 2, a deleterious, RNA gain-of-function model for DM1 involves the CUG^{exp} transcript sequestering the alternative splicing regulator, muscleblind-like 1 (MBNL1) into nuclear foci, which leads to splicing defects in >100 pre-mRNAs.⁸

Received: April 10, 2016

Published: June 29, 2016

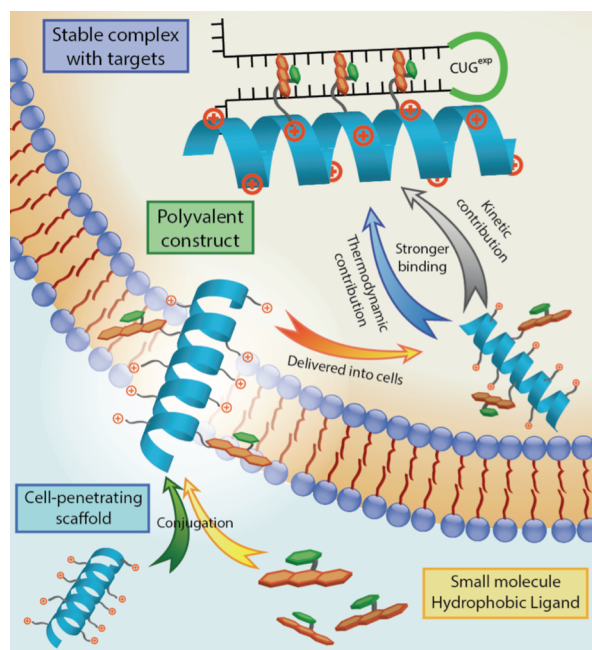


Figure 1. Schematic illustration of the polymeric approach for the fabrication of multivalent construct with synthetic polypeptide having dual function as scaffold and transporter. The stability of the complex formed between the multivalent ligand and the target RNA are improved both kinetically and thermodynamically.

One therapeutic strategy has focused on cell-permeable small molecules that selectively inhibit the transcription of CTG^{exp} or bind CUG^{exp} and inhibit MBNL sequestration.⁹ As described above, the repeating nature of the DNA and RNA target means that linking two or more of these monomeric ligands can produce a multivalent effect, resulting in enhanced selectivity and affinity.^{4b,10} Indeed, compounds with nanomolar K_i values for inhibiting CUG^{exp} -MBNL1 complex are now known, but these often show partial rescue of pre-mRNA mis-splicing in the DM1 model cells or require relatively high concentrations (10–100 μM) for full rescue.¹⁰ These findings may indicate that cell permeability limits the compound activity. Herein, we report the use of a synthetic cell-penetrating peptide (CPP) mimic¹¹ to function as both a delivery vehicle for transmembrane transport and as a scaffold to display multiple copies of a CUG^{exp} -selective ligand (Figure 1). By combining these two functions, a series of tunable polymeric, multivalent DM1 ligands are readily available that exhibit significantly improved efficacy in a DM1 cell model, showing low nanomolar K_i values and high splicing rescue of insulin receptor (*IR*) pre-mRNA at low concentrations. The polymers were tested *in vivo* using a DM1 *Drosophila* larval crawling assay and a significant improvement in the pathogenic phenotype was observed.

EXPERIMENTAL SECTION

Materials and Methods. All reagents were purchased from Acros Organics, Fisher Scientific, AK Scientific, TCI America, or Sigma-Aldrich, and used without further purification unless otherwise noted. Water was obtained from a Milli-Q purification system. Instrument setup and synthetic procedures for small molecules, polymers, and

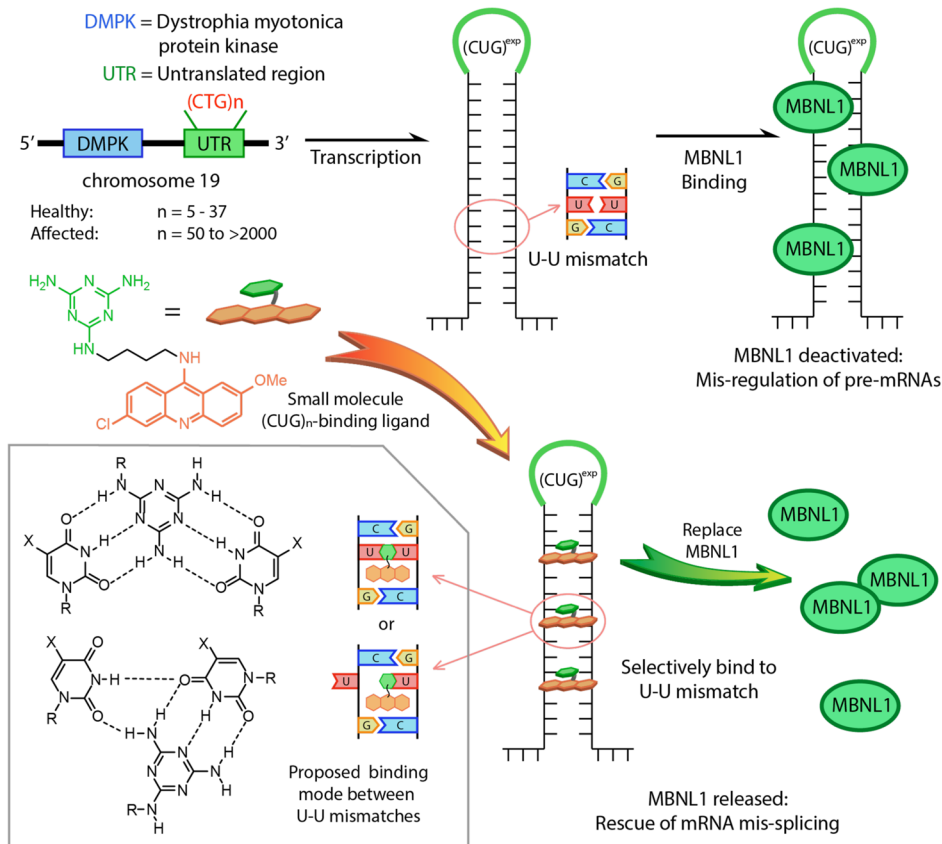


Figure 2. Proposed mechanism for how CTG expansion in *DMPK* gene leads to DM1, and a simple illustration of how acridine-melamine small molecule targets CUG^{exp} , selectively inhibiting formation of MBNL1- CUG^{exp} RNA complexes.

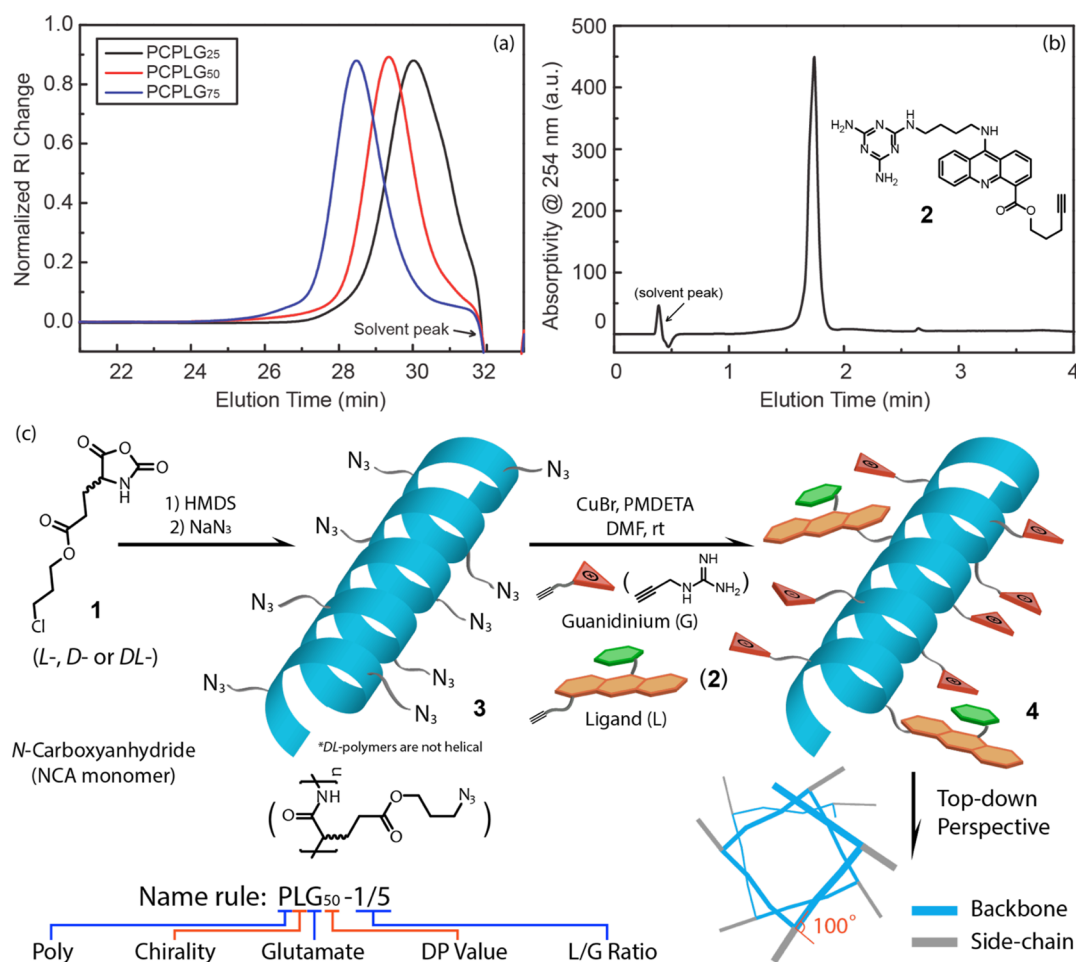


Figure 3. (a) GPC curve overlay of parent polymers, poly[γ -(3-chloropropyl)-L-glutamates] (PCPLGs), of three different molecular weights. PDI < 1.10 for all three. These results are typical for the polymers studied. (b) HPLC elution curve of the alkyne-bearing DM1 ligand using C-18 reverse-phase column and gradient elution from solvent A/B = 20/80 to 80/20; solvent A = CH₃CN, solvent B = H₂O with 0.1% TFA. (c) Synthesis of the polymeric ligand in schematic format. The guanidinium and acridine moieties on the side-chains are placed on the exterior of the α -helical polypeptide rod, as visualized by the top-down view.

proteins as well as methods used to determine the bioactivity of the polymeric ligands can be found in the [Supporting Information](#).

RESULTS AND DISCUSSION

Synthesis of the Polypeptide-based DM1 Polymeric Ligands. In selecting a membrane-penetrating polymer to serve as a scaffold for multiligand display, there were many options. The guanidinium-rich polypeptide system recently developed by Cheng and co-workers¹² was selected because of its accessibility and defined structure. In particular, these α -helical polymers can be synthesized using a facile and controlled living polymerization of *N*-carboxyanhydride (NCA) 1. The product polyazide has the potential for multiple postfunctionalization reactions using the copper(I)-catalyzed alkyne–azide cycloaddition (CuAAC).¹³ The synthesis of 1 generally followed the reported approach.^{14,15} Thus, the functionalized amino acids, γ -(3-chloropropyl)-L-glutamate, γ -(3-chloropropyl)-D-glutamate and γ -(3-chloropropyl)-DL-glutamate, were prepared by acid-catalyzed esterification of 3-chloro-1-propanol and the corresponding glutamic acid (L-, D-, or DL-isomer). Treatment with phosgene in THF afforded the corresponding γ -(3-chloropropyl)-L-, D-, and DL-glutamic acid *N*-carboxyanhydrides (L-, D-, and DL-Glu-NCA). For the ligand, we selected acridine-melamine conjugate 2, which is an alkyne-

containing derivative of a ligand reported by Baranger and Zimmerman in 2009 to selectively bind CUG^{exp} with high nanomolar affinity.^{9c}

The polymerization of 1 was effected using hexamethyldisilazane (HMDS) as the initiator¹⁶ to give the corresponding polypeptides, namely poly[γ -(3-chloropropyl)-L-glutamate] (PCPLG), poly[γ -(3-chloropropyl)-D-glutamate] (PCPDG), and poly[γ -(3-chloropropyl)-DL-glutamate] (PCPDLG). The degree of polymerization (DP) of polypeptide is controlled by monomer-to-initiator (M/I) feed ratio. As seen in [Figure 3a](#), the GPC traces for PCPLGs prepared with 1:25, 1:50, and 1:75 initiator to monomer ratios gave symmetrical peaks with decreasing retention times. In each case, the polydispersity index (PDI) was <1.10. The stereochemistry of the amino acid residues on each polypeptide (L-, D-, or DL-) was determined by the NCA monomer used. The side-chain chloro groups were converted to azido groups by treatment with NaN₃ in DMF giving polyazide 3. In each case, the chloride to azide conversion appeared to be quantitative based on the ¹H NMR characterization (Figures S4 and S5 in [Supporting Information](#)) giving poly[γ -(3-azidopropyl)-L-glutamate] (PAPLG), poly[γ -(3-azidopropyl)-D-glutamate] (PAPDG), and poly[γ -(3-azidopropyl)-DL-glutamate] (PAPDLG).

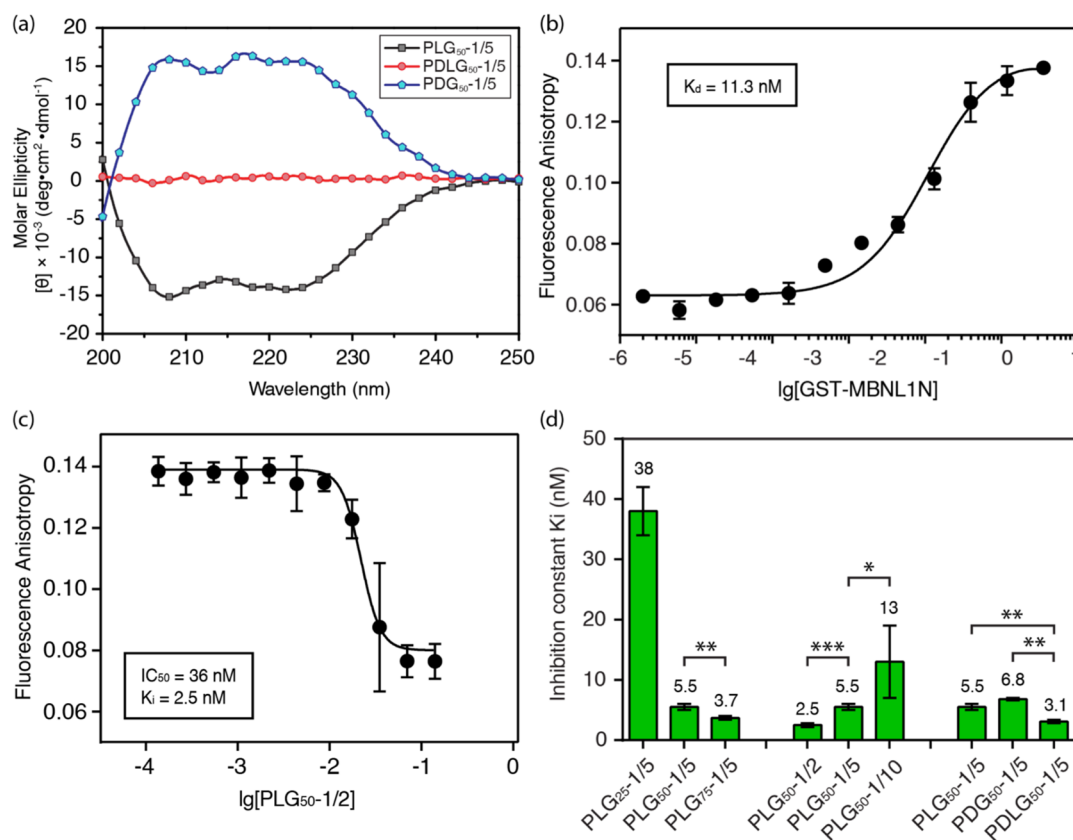


Figure 4. (a) CD spectra of PLG₅₀-1/5, PDG₅₀-1/5, and PDLG₅₀-1/5 (aqueous solution). The L- and D-polymers showed characteristic double minimum or maximum for helical polypeptides at 208 and 222 nm. On the contrary, the DL-polymers did not show any helicity. (b) Measurement of dissociation constant of GST-MBNL1N-(CUG)₁₆ complex by fluorescence anisotropy and curve-fitting. (c) Representative fluorescence anisotropy titration curve of the polymeric ligand (PDLG₅₀-1/2) and the corresponding IC_{50} and K_i calculated. Studies of other polymeric ligands were performed analogously. (d) Summary of measured K_i of all polymeric ligands. * indicates $P \leq 0.05$; ** indicates $P \leq 0.01$; and *** indicates $P \leq 0.001$ as determined by a two-tailed Student's *t*-test.

The azido-rich polypeptides served as the parent polymers for the conjugation of *N*-propargylguanidine, ligand 2 (Figure 3b), and an RNAzyme-mimicking pentapeptide (*vide infra*).¹⁷ A schematic illustration of the synthesis of polymeric, multivalent ligands 4 is shown in Figure 3c. The Cu(I) catalyzed alkyne-azide cycloaddition is both a highly chemoselective and high yielding reaction, so the conjugation was considered likely to be quantitative and the ratio of side-chains to be equal to the reagent stoichiometry. Support for this assumption came from several observations, including a characteristic triazole peak in the ¹H NMR (Figure S6). The acridine resonances were not observed possibly because packing of the hydrophobic chromophores within the helix leads to their reduced mobility (slow tumbling) and poor solvation.^{18,19} The ligand incorporation into the polymers was established by the acridine fluorescence observed for each polymer, and particularly by UV studies that showed an approximately linear increase in absorbance with L/G feed ratio (Figure S3). The molecular weight of each polymer 4 was calculated based on the molecular weight of parent PCPLGs determined by multiangle laser light scattering (MALLS) and the alkyne loading stoichiometry (Table S1).

Homochiral Polymers are Charged Helical Rods. The α -helical structure of multivalent ligand 4 is an essential design feature by (1) incorporating cell membrane permeability and (2) maintaining the ligands on the exterior of the helical rod and available for binding. The CD spectra of PLG₅₀-1/5,

PDG₅₀-1/5, and PDLG₅₀-1/5 are shown in Figure 4a. Note that the naming convention of the polymeric agents is outlined in Figure 3, with P referring to polymer, D, L, or DL the chirality of the monomeric units, G the glutamate monomer unit, the subscript the degree of polymerization, and the ratio of ligand to guanidinium side-chain. For PLG₅₀-1/5, a characteristic double minimum at 208 and 222 nm was observed, indicating that the ligand-loaded polypeptide adopts a standard helical structure. Using eq 1 (see Experimental section in SI), the helicity % was estimated to be approximately 50%. For PDG₅₀-1/5, prepared from the D-monomers, positive bands at 208 and 222 nm were observed in the CD spectrum of PDG₅₀-1/5, closely resembling a mirror image of the spectrum of PLG₅₀-1/5. In contrast, the random D-/L-copolymer, PDLG₅₀-1/5, showed a flat curve near the baseline, indicating a random coil structure with no Cotton effect.

Computational studies²⁰ have shown this class of polymers to have hindered, hydrophobic backbones that reside in a water-depletion zone and, indeed they have been shown to be significantly more stable to enzymatic cleavage by peptidases.²¹ It was anticipated that the esters would be similarly protected from cytosolic esterases and, indeed, porcine liver esterase (PLE), which has a broad substrate scope showed no cleavage of PLG₅₀-1/5 over a 72 h period (Figure S8 in Supporting Information). With this set of stable polymers containing different chirality, it was possible to determine the importance of the helical structure to be established.

Polymers Are Potent *in Vitro* Inhibitors of the MBNL1-r(CUG)₁₆ Interaction Exhibiting Nanomolar K_i Values. To assess the ability of the polymeric ligands to inhibit the MBNL protein sequestration by CUG^{exp}, fluorescence anisotropy inhibition experiments were performed using GST-MBNL1 protein²² and TAMRA-labeled r(CUG)₁₆ (see Supporting Information).²³ Figure 4b shows the change in fluorescence anisotropy upon titration of TAMRA-r(CUG)₁₆ with GST-MBNL1. Curve fitting gave a dissociation constant (K_d) for the protein-RNA complex, $K_d = 11.3$ nM, which is close to that reported previously.²²

To measure the inhibition potential of the polymeric ligands, the [GST-MBNL1]·[TAMRA-r(CUG)₁₆] complex (abbreviated as MBNL1-r(CUG)₁₆) was titrated with the polymeric ligand (Figure 4c). Curve fitting the plot of fluorescence anisotropy against the polymeric ligand concentration afforded IC_{50} and K_i values that were in the low nanomolar range. The comparative performance of the various polymeric ligands is shown graphically in Figures 4d and S10. Similar to the trend reported by Kiessling and co-workers for glycopolymers,²⁴ a higher ligand loading generally led to lower K_i values. PLG₅₀-1/5 and PDG₅₀-1/5 showed similar K_i values, indicating that the chirality of α -helix plays a minor role in the peptide-RNA binding. Interestingly, PDLG₅₀-1/5 showed improved IC_{50} and K_i , indicating that the recognition units are still very much available for binding. The increased ability of PDLG₅₀-1/5 to inhibit the MBNL1-r(CUG)₁₆ complex likely results from the random-coil conformation of the polypeptide allowing for a flexible fit between macromolecules. However, as shown in the confocal studies (*vide infra*), PDLG₅₀-1/5 was not as cell permeable as the helical polymers.

As noted above, the binding affinity and inhibition potency of the polymeric ligands were seen to increase with the acridine-melamine loading on the polymer. Although further improvements in inhibition potency may be observed by further increasing ligand loading, solubility or aggregation of the resulting polymeric constructs is likely to be an issue. Thus, decreased aqueous solubility was observed for PLG₅₀-1/2 compared to PLG₅₀-1/10 and PLG₅₀-1/5, although PLG₅₀-1/2 was still soluble enough for all studies. Increasing the polymer length is another approach to increase the multivalency, but that approach raises concerns about the synthetic accessibility and ultimately the issue of body clearance.

Confocal Microscopy Shows Polymeric Ligands are Taken up by HeLa Cells. Confocal microscope images of live HeLa cells treated with the DM1 polymeric ligands 4 provided semiquantitative evidence of the ability of the polymeric ligand to pass the cell membrane and at least partially enter the nucleus. The results for PLG₅₀-1/5, PDG₅₀-1/5, and PDLG₅₀-1/5 are shown in Figure 5. The polymers containing D- or L-monomers exclusively showed better cellular uptake relative to the DL-polymer consistent with cell penetration mediated by the helical structure.^{12b} The helical polypeptides were observed in the endosome, cytoplasm, and some in the nucleus of cells. It was reported that hydrophobic groups such as alkyl chains on PLG are necessary for better cellular uptake, and the uptake process is governed by both endocytosis and direct penetration.^{12b} In this work, the acridine-melamine ligands likely provide the hydrophobic moieties, although they led to more uptake by the endocytosis pathway (Figure S11).

The cell uptake results underline the importance of using a suitable vector for ligands to be transported into the cells to find their target. Although CPP-like functionality has not yet

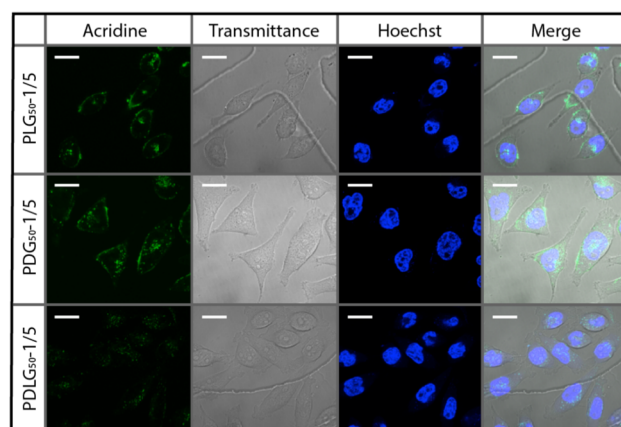


Figure 5. HeLa cellular uptake studies with PLG₅₀-1/5, PDG₅₀-1/5 and PDLG₅₀-1/5 monitored by confocal microscopy of live cells. Hoechst dye was used as a nuclear stain (blue). The acridine moieties on the polypeptide showed inherent fluorescence (green), allowing the location of the polymer–ligand conjugates to be determined. Incubation time was 4 h with a ligand concentration of 500 nM. Scale bar = 20 μ M.

found use in the clinic, CPP-conjugated oligonucleotides are being investigated as potential treatments of various muscular dystrophies.²⁵ In this study that target is the expanded rCUG transcript located in the nucleus. The random-coiled DL-polymer showed less uptake by the HeLa cells. Thus, despite the better inhibition potency observed in the *in vitro* fluorescence anisotropy studies, these ligands are less attractive as agents for treating DM1. Moreover, helicity is not only important for cell-penetrating capability, but also affecting the ultimate fate of the polymer. Although beyond the scope of this study, the D-polypeptides are expected to resist enzymatic degradation. It is likely that long-term toxicity and clearance rates will depend on the chirality. Beyond whether D- or L-monomers are used, the synthesis outlined in Figure 3c is sufficiently flexible to allow other functionality to be added and the many different structural parameters to be varied in a systematic way.

Nuclear Foci Formation Is Inhibited in Model DM1 Cells by Polymeric Ligands. One of the hallmarks of DM1 is the formation of nuclear foci, resulting from MBNL sequestration by CUG^{exp}.²⁶ These foci can be readily visualized by confocal microscopy. In this study, DM1 model cells were constructed by transfecting HeLa cells with a GFP-DT960 plasmids²⁷ containing (CTG)₉₆₀ in a truncated *DMPK* gene and a sequence encoding GFP protein to assess the transfection efficiency.

PLG₅₀-1/5 was used in the initial study along with PLG₅₀-0/1, a control polymer lacking acridine ligands. In the untreated cells, the colocalization of Cy3-(CAG)₁₀ and an anti-MBNL antibody led to the visualization of nuclear foci (Figure 6). In contrast, cells treated with 500 nM PLG₅₀-1/5 for 2 d showed fewer foci, and their sizes were noticeably smaller (Figure 6, row 3). No significant change in the foci number was observed for the cells treated with the control polymer (PLG₅₀-0/1) under the same conditions (Figure 6, row 2). These results revealed the importance of the CUG^{exp}-binding moieties on the polypeptides. In addition, the working concentration of the polymeric ligand PLG₅₀-1/5 (500 nM) was 2 orders of magnitude lower than that of the monomeric small molecule

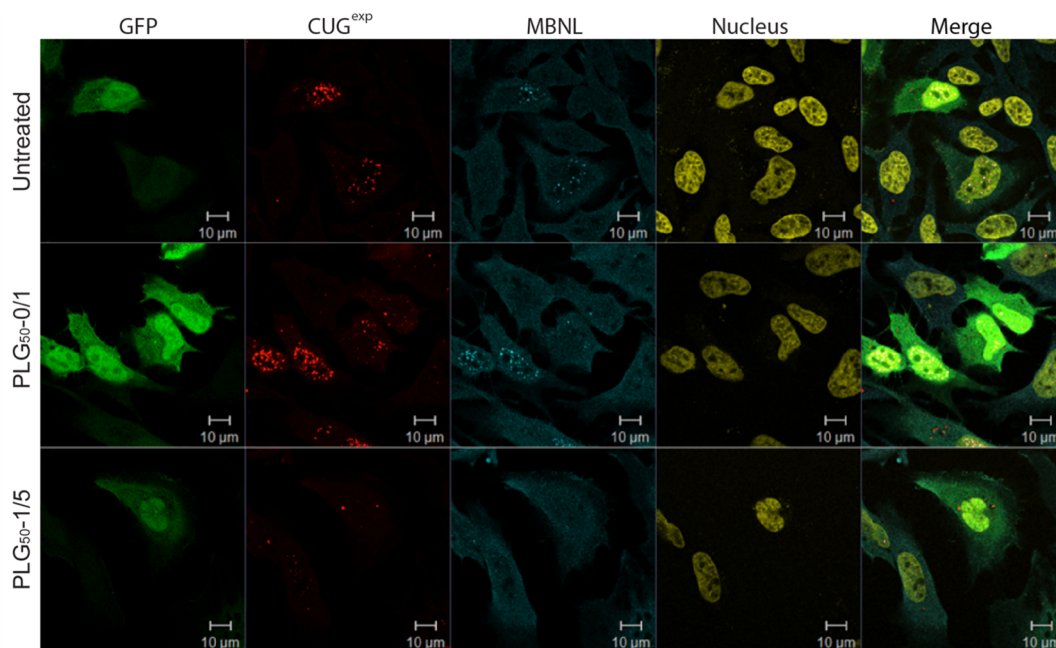


Figure 6. Reduction of nuclear foci in the DM1 model cells were observed by treating the cells with 500 nM polymeric ligand (PLG₅₀-1/5). Control polymer (without ligand conjugated) showed no efficacy.

ligand (50 to 100 μ M),^{19,22} showing a significant improvement in efficacy for this rationally designed polymeric ligand system.

The IR Pre-mRNA Mis-Splicing Is Fully Corrected by the Polymeric Ligands in DM1 Model Cells. Given the ability of the polymers to inhibit foci formation and sequestration of MBNL1, the downstream effect on splicing mis-regulation was examined in DM1 model cells constructed by cotransfecting HeLa cells with plasmids containing (CTG)₉₆₀ (DT960) and the IR minigene. The splicing of IR pre-mRNA was chosen for study because it is relatively difficult to be rescued.²⁸ As seen in Figure 7a, the IR pre-mRNA undergoes splicing to form two isoforms, A and B, the former without and the latter with exon 11 included.

The DM1 model cells were treated with polymeric ligands at concentrations where high levels of foci dispersion and cell viability were observed. The relative amounts of two IR isoforms were measured for treated and untreated cells. The splicing of IR pre-mRNA in untreated HeLa cells containing the IR minigene, but lacking the DT960 minigene, produced ca. 47% of isoform B, whereas the DM1 model cell produced only 27% (Figure 7b). These differences in the levels of the IR isoforms generally reproduce that observed in normal and DM1 patient cells.²⁹ Treatment of the DM1 model cells with the polymeric ligands reversed the splicing defect of IR pre-mRNA to within experimental error of normal cells (Figures 7b and S12). Ligand PLG₅₀-1/2 appeared to be most effective giving full rescue at ≤ 225 nM, but all ligands studied corrected the splicing defect at concentrations from 0.1 to 1 μ M (Figure S12). In comparison to other small molecules that target CUG^{exp},²² the polymeric ligands exhibited significantly higher activity.

Polymeric Ligands Exhibit Acceptable Cytotoxicity. Minimal cell death was observed during the splicing recovery and foci dispersion experiments described above and at a level that was indistinguishable from the control using no compound. Indeed, the parent CPP-mimicking polypeptides used here were reported to have relatively low toxicity.^{12b}

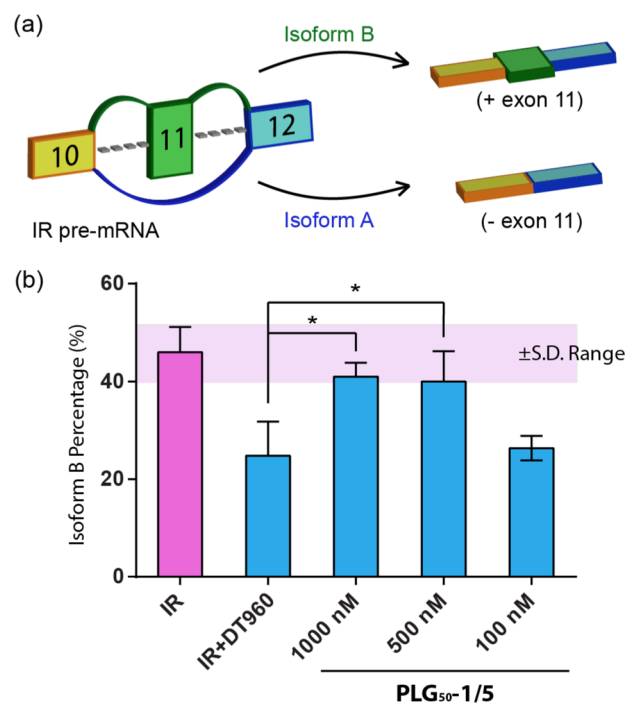


Figure 7. Reversal of IR mis-splicing with DM1 polymeric ligand. (a) Schematic illustration of the splicing of IR pre-mRNA. (b) Results from three concentrations of PLG₅₀-1/5 after 72 h incubation. Error bars represent standard error of the mean of the three independent experiments. * $P < 0.05$ (two-tailed Student's t -test).

Nonetheless, the cytotoxicity of polymer 4 at their respective working concentrations was evaluated using multiple cell lines, including DM1 patient cells (see Figure S13). The results showed that 4 exhibited no or relatively low cytotoxicity at their working concentrations of 225 nM for PLG₅₀-1/2, 500 nM for PLG₅₀-1/5, and 1 μ M for PLG₅₀-1/10. The cytotoxicity of 4 with HEK-293 cells at higher polymer concentrations was also

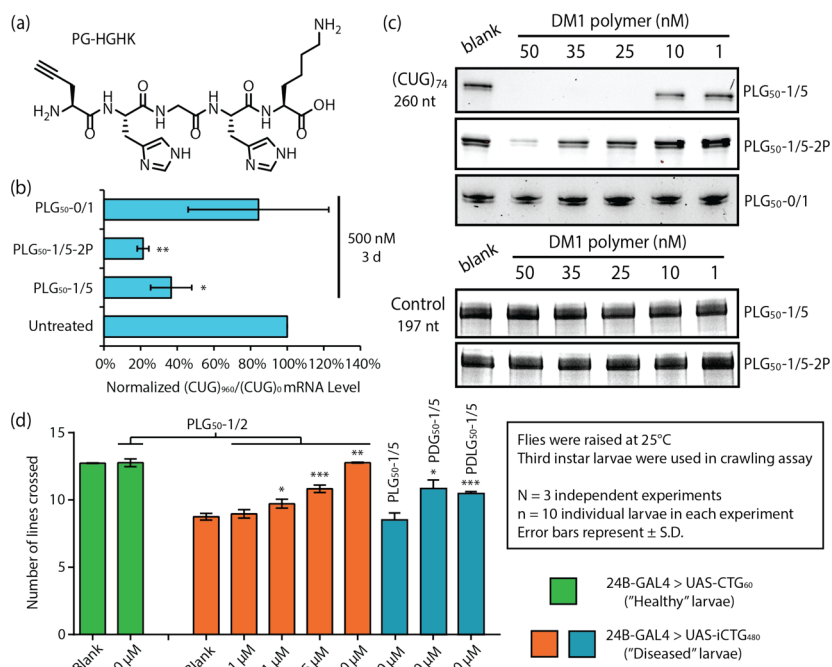


Figure 8. (a) Structure of alkyne-containing pentapeptide that, along with **2** and *N*-propargyl guanidine was conjugated to **3** to produce a potential RNA-cleaving **4**. (b) Change in CUG^{exp} levels in DM1 model cells after 3 d treatment of polymeric ligands PLG₅₀-1/5 and PLG₅₀-1/5-2P. The error bar represent standard error of mean from at least three independent experiments, * *P* < 0.05, ** *P* < 0.01, *** *P* < 0.001 (two tailed *t*-test). (c) *In vitro* transcription experiments using a linearized plasmid containing (CTG-CAG)₇₄ and control plasmids in the presence of DM1 polymers. (d) Dose-dependent rescue (PLG₅₀-1/2) and the effect of polymer chirality (PLG₅₀-1/5, PDG₅₀-1/5 and PDLG₅₀-1/5) on the rescue of locomotion defect in DM1 larvae at low concentration in the larval food. See text, Supporting Information, and ref 9h for additional details.

examined in an effort to understand the relationship between the polymer structure and its toxicity (Figure S14). The more hydrophobic polymer, PLG₅₀-1/2, showed higher toxicity at higher concentrations compared to other polymers. This possibly resulted from the higher loading of the hydrophobic ligands on the polymer backbone, which may lead to more aggressive cell membrane disruption that compromises membrane integrity, leading to cell death.^{12b,30} Nonetheless, the higher inhibitory power of PLG₅₀-1/2 allows for lower dosing, and it showed excellent activity in the foci and splicing assays along with PLG₅₀-1/5 and PLG₅₀-1/10 without significantly affecting model cell viability.

Polymeric Ligands Suppress Cellular Levels of CUG^{exp} RNA Transcript. The DM1 disease pathobiology is complex, and the CUG^{exp} may produce additional toxicity beyond the sequestration of MBNL. For example, CUG^{exp} undergoes repeat-associated non-ATG (RAN) translation producing homopeptides, some of which are known to be toxic.³¹ The CUG^{exp} transcript also disrupts the translation of MEF2 protein, leading to microRNA dysregulation in DM1 heart tissue.^{27b,32} For these reasons, ligands that suppress CUG^{exp} levels may be superior to those that simply inhibit MBNL1 sequestration. We recently reported several small molecules that target DM1 simultaneously through three separate pathways.³³ In particular, these multitargeting agents were shown *in vitro* to (1) inhibit the transcription of the expanded dCTG DNA, (2) slowly and selectively cleave CUG^{exp}, and (3) inhibit the formation of the CUG^{exp}-MBNL complex. One or both of the first two capabilities likely led to the reduced CUG^{exp} levels observed in DM1 model cells.

Taking advantage of the ease in synthesis, a potential RNA-cleaving pentapeptide (propargyl-glycine-His-Gly-His-Lys) was incorporated into the polymeric ligand (Figure 8a). This

pentapeptide is a clickable derivative of a tetra-peptide, HGHK, whose acridine conjugate was reported to cleave tRNA under physiological conditions.³⁴ The new polymeric ligand, PLG₅₀-1/5-2P, was prepared using the same synthetic approach outlined in Figure 3a. PLG₅₀-1/5-2P had an acridine-melamine to guanidine ratio of 1:5 and an average of two pentapeptides per polymer chain. CD spectroscopy was used to show that the attached pentapeptides did not disrupt the helical structure of the polypeptide (Figure S15a). Cell uptake studies using PLG₅₀-1/5-2P revealed an uptake profile similar to that of PLG₅₀-1/5 (Figure S15b).

To examine the potential for these ligands to regulate the cellular levels of CUG^{exp}, the two polymeric ligands, PLG₅₀-1/5 and PLG₅₀-1/5-2P, were studied using the same DM1 model cells described above containing GFP-DT960. The model cells were incubated with 500 nM of the polymeric ligands for 3 d. The total RNA was isolated, and the r(CUG)₉₆₀ mRNA level was determined by measuring the mRNA levels of exon 15 upstream of CUG^{exp} using PABP mRNA as an internal standard.³³ The results shown in Figure 8b indicate that the toxic mRNA level was decreased by over 75% for both polymers, with PLG₅₀-1/5-2P outperforming PLG₅₀-1/5. The possibility that the ligands, if isolated with the RNA, might interfere with cDNA synthesis and amplification of the target mRNA was ruled out in control experiments. Thus, the presence of polymeric ligands in a concentration range of 0.5–500 nM showed no effect on the reverse transcription or RT-PCR reactions (see Figure S16), ruling out the possibility of a false positive response resulting from this type of interference.

The two possible mechanisms that account for the observed suppression of the rCUG transcript levels are (1) inhibition of (CTG)₉₆₀ transcription and (2) degradation of the r(CUG)₉₆₀ transcript. To better understand the regulation mechanism, *in*

in vitro transcription inhibition experiments using a (CTG)₇₄-containing DNA template were performed in the presence of PLG₅₀-1/5 and PLG₅₀-1/5-2P. Thus, linearized T7 promoter-containing (CTG)₇₄ plasmids³⁵ were incubated for 2 h with T7 polymerase in the presence of polymeric ligands PLG₅₀-1/5 and PLG₅₀-1/5-2P at concentrations ranging from 1 nM to 500 nM. The results showed that PLG₅₀-1/5 and PLG₅₀-1/5-2P significantly inhibited r(CUG)₇₄ formation at a concentration as low as 50 nM (>70% inhibition, Figures 8 and S17), whereas the control polymer PLG₅₀-0/1 showed little inhibition at all testing conditions. A dose-dependent effect of the ligands on *in vitro* transcription was observed. In contrast, there was no clear trend seen for control polymer PLG₅₀-0/1, indicating the need for the acridine ligand to selectively recognizing CTG DNA.^{9c,h} Consistent with this model, PLG₅₀-1/5 and PLG₅₀-1/5-2P showed no effect on the *in vitro* transcription of a control sequence lacking the (CTG-CAG)₇₄ sequence (Figure 8c).

In a parallel experiment, PLG₅₀-1/5-2P was incubated with r(CUG)₇₄ under the same conditions without the DNA template. No RNA degradation was observed over a 2 h incubation (Figure S18) suggesting that the decreased level of r(CUG)₇₄ in the transcription experiments originates primarily in the inhibition of transcription, not RNA degradation. However, over longer periods both PLG₅₀-1/5 and PLG₅₀-1/5-2P showed r(CUG)₁₆ cleavage. Thus, ³²P-labeled r(CUG)₁₆ showed smaller RNA fragments after a 24 h incubation with either PLG₅₀-1/5 or PLG₅₀-1/5-2P (Figure S19). Given that the cell studies used a 3 d incubation, it is possible that RNA cleavage contributes to the suppression in CUG RNA levels. However, it is beyond the scope of this study to determine the relative importance of transcription inhibition relative to the RNA cleavage.

Polymer PLG₅₀-1/2 Fully Corrects the Mobility Defect of DM1 Transgenic *Drosophila* Larvae. The expression of expanded CUG repeats in *Drosophila* was reported to lead to nuclear accumulation of CUG RNA, splicing misregulation, and lowered MBNL function, with reduced lifespan and muscle degeneration.³⁶ A larval crawling assay was initially developed by Pandey and co-workers for ALS modeling, as motor neuron expression of mutant FUS/TLS was observed to cause a larval-crawling defect.³⁷ Based on the above studies, we recently developed a DM1 *Drosophila* larval crawling assay and used it to examine the *in vivo* activity of two bisamidinium compounds.³³ Thus, the locomotion of transgenic larvae expressing either an uninterrupted (CTG)₆₀ or an interrupted (CTG)₄₈₀ sequence was measured by placing them on an agarose gel dish over grid paper and recording the number of lines crossed per minute. The transgenic larvae expressing (CTG)₆₀ crossed ~12.5 lines/min, which is considered to be the nonpathogenic control, whereas those expressing i(CTG)₄₈₀ exhibited significantly impaired locomotion, crossing ~9 lines/min (pathogenic state). The same assay was used to test the *in vivo* activity of the polymeric ligands developed herein, the data summarized in Figures 8d and S20.

The six polymers studied showed minimal effect on the mobility of the control (nonpathogenic) transgenic larvae containing (CTG)₆₀ (Figures 8d and S20). Of the six ligands investigated, three showed significant improvement in the crawling defect of the i(CTG)₄₈₀ larvae, and of these, PLG₅₀-1/2 showed the largest effect. As seen in Figure 8d, PLG₅₀-1/2 exhibited a dose-dependent response with larval mobility fully recovered to nonpathogenic levels at 10 μM. Although this polymer exhibited the highest cytotoxicity in HEK-293 cells

among all the synthesized polymers, it also showed the highest activity in inhibiting the MBNL1·r(CUG)₁₆ interaction *in vitro*. In addition, the three polymers with similar structure but different chirality, PLG₅₀-1/5, PDG₅₀-1/5, and PDLG₅₀-1/5, showed a clear trend in locomotive ability rescue capability: PDG₅₀-1/5 > PDLG₅₀-1/5 > PLG₅₀-1/5, which correlates with their anticipated resistance to enzymatic degradation across the longer time frame of the *in vivo* experiments: PDG₅₀-1/5 > PDLG₅₀-1/5 > PLG₅₀-1/5. In fact, no activity was observed for L-peptides of lower ligand loading at the tested concentration (10 μM). There are many factors that will determine the *in vivo* activity, including the amount of agent consumed in feeding as well as its absorption, distribution, and metabolism. Additional studies would be needed to determine if the D-chirality is correlated with increased *in vivo* stability, and in turn, this accounts for the higher activity.

CONCLUSION

Amplifying the affinity and selectivity of ligands that target trinucleotide repeat diseases can be accomplished logically by linking two or more of these ligands together with the appropriate scaffold. However, these multivalent ligands must be taken up by the cell and the larger the multivalent construct, often the more difficult it is to achieve suitable uptake. This study reports a general strategy to avoid this limitation. In particular, we described the first approach toward DM1 treatment that uses a polymeric delivery agent, a cell-penetrating peptide mimic, as the scaffold to bring multiple CTG- and CUG-binding agents to the target DNA and RNA within the cell. Although the cellular and *in vivo* fate of these macromolecular constructs is unknown and one cannot rule out the possibility of enzymatic ester or peptide cleavage, the >100 fold increase in potency, known peptidase resistance of these polymers,²¹ and demonstrated resistance to esterase cleavage are more consistent with a multivalent mode of action.

Despite the complexity of the construct, its synthesis was straightforward using a bottom-up, living polymerization strategy. Polyazide 3 allowed different loadings of various ligands and other groups to be easily linked to the scaffold providing considerable tunability. By preparing a series of DM1 polymeric ligands with different molecular weights (i.e., chain lengths), ligand loadings and helicity, the effects of these parameters could be evaluated in both *in vitro* and *in vivo* assays. Further improvements in the inhibition power and therapeutic efficacy could come from even more controlled structural variants, such as those biasing the CUG ligands to one side of the helical rod, or with precise control over distance between each CUG-targeting ligand on the rod. Both approaches would help optimize the multivalent effect. Alternatively, an oligomeric ligand with optimized distance between each binding units may be conjugated to a TAT-like CPP to achieve similar improvements in efficacy.

Synthetic polypeptide-based ligands (e.g., PLG₅₀-1/5) were shown to perform well in the DM1 model cells. Thus, they significantly inhibited the formation of nuclear foci at concentrations of 500 nM and fully or nearly fully reversed the mis-splicing of the *IR* pre-mRNA in the DM1 model cells at ≤1 μM. PLG₅₀-1/5 and PLG₅₀-1/5-2P were shown to be multitargeting agents. Thus, beyond inhibiting the MBNL1·CUG^{exp} interaction both significantly inhibited (CUG)_n formation at concentrations as low as 50 nM (>70% inhibition). Mechanistic studies showed that both PLG₅₀-1/5 and PLG₅₀-1/5-2P acted as selective inhibitors of CTG

transcription. This activity was unsurprising given that the melamine-acridine ligand was reported to bind CTG sites in DNA and CUG sites in RNA with similar affinity ($K_d \sim 400$ nM).^{9c,h} Three of the six ligands studied, exhibited significant phenotypic improvement in a DM1 *Drosophila* larvae crawling assay, with PLG₅₀-1/2 showing full correction of the crawling defect.

In a broader sense, the use of a cell-penetrating peptide as a scaffold for generating a multivalent ligand display may be more generally applied, not only to other TREDs but also to any intracellular target that could benefit from a similar polyvalent strategy.

■ ASSOCIATED CONTENT

Supporting Information

The Supporting Information is available free of charge on the ACS Publications website at DOI: 10.1021/jacs.6b03697.

Detailed instrument setup, synthetic procedures, additional polymer characterization data, additional protocols for molecular and cell studies, and additional supportive experiments (PDF)

(MOV)

(MOV)

(MOV)

(PDF)

■ AUTHOR INFORMATION

Corresponding Author

*sczimmer@illinois.edu

Author Contributions

[†]These authors contributed equally.

Notes

The authors declare no competing financial interest.

■ ACKNOWLEDGMENTS

Funding from the Muscular Dystrophy Association (MDA grant 295229 to S.C.Z.) and the National Science Foundation (CHE 1153122 to J.C.) is gratefully acknowledged. The authors thank Auinash Kalsotra (University of Illinois at Urbana-Champaign, Urbana, IL) for the GFP-DT0 and GFP-DT960 plasmids, Thomas Cooper (Baylor College of Medicine, Houston, TX) for the DT960 minigene plasmid, Maurice Swanson (University of Florida, Gainesville, FL) for the (CTG)₇₄ plasmid, and Nicholas Webster (University of California, San Diego, CA) for the IR minigene plasmid.

■ REFERENCES

(1) (a) Mammen, M.; Choi, S.-K.; Whitesides, G. M. *Angew. Chem., Int. Ed.* **1998**, *37*, 2754–2794. (b) Kiessling, L. L.; Gestwicki, J. E.; Strong, L. E. *Curr. Opin. Chem. Biol.* **2000**, *4*, 696–703. (c) Lundquist, J. J.; Toone, E. J. *Chem. Rev.* **2002**, *102*, 555–578. (d) Levine, P. M.; Carberry, T. P.; Holub, J. M.; Kirshenbaum, K. *MedChemComm* **2013**, *4*, 493–509. (2) Selected examples: (a) Gestwicki, J. E.; Cairo, C. W.; Strong, L. E.; Oetjen, K. A.; Kiessling, L. L. *J. Am. Chem. Soc.* **2002**, *124*, 14922–14933. (b) Patke, S.; Boggara, M.; Maheshwari, R.; Srivastava, S. K.; Arha, M.; Douaisi, M.; Martin, J. T.; Harvey, I. B.; Brier, M.; Rosen, T.; Mogridge, J.; Kane, R. S. *Angew. Chem., Int. Ed.* **2014**, *53*, 8037–8040. (c) Hollenbeck, J. J.; Danner, D. J.; Landgren, R. M.; Rainbolt, T. K.; Roberts, D. S. *Biomacromolecules* **2012**, *13*, 1996–2002. (d) Craig, P. O.; Alzogaray, V.; Goldbaum, F. A. *Biomacromolecules* **2012**, *13*, 1112–1121. (e) Englund, E. A.; Wang, D.; Fujigaki, H.; Sakai, H.; Micklitsch, C. M.; Ghirlando, R.; Martin-Manso, G.; Pendrak, M. L.; Roberts, D.

D.; Durell, S. R.; Appella, D. H. *Nat. Commun.* **2012**, *3*, 614. (f) Yang, L.; Meng, L.; Zhang, X.; Chen, Y.; Zhu, G.; Liu, H.; Xiong, X.; Sefah, K.; Tan, W. *J. Am. Chem. Soc.* **2011**, *133*, 13380–13386. (g) Thomas, T. P.; Huang, B.; Choi, S. K.; Silpe, J. E.; Kotlyar, A.; Desai, A. M.; Zong, H.; Gam, J.; Joice, M.; Baker, J. R. *Mol. Pharmaceutics* **2012**, *9*, 2669–2676.

(3) Selected examples: (a) Krishnamurthy, V. M.; Estroff, L. A.; Whitesides, G. M. In *Fragment-based Approaches in Drug Discovery*; Wiley-VCH Verlag GmbH & Co. KGaA: Weinheim, 2006; p 11–53. (b) Choi, S.-K.; Mammen, M.; Whitesides, G. M. *J. Am. Chem. Soc.* **1997**, *119*, 4103–4111. (c) Kiessling, L. L.; Pohl, N. L. *Chem. Biol.* **1996**, *3*, 71–77. (d) Becer, C. R.; Gibson, M. I.; Geng, J.; Ilyas, R.; Wallis, R.; Mitchell, D. A.; Haddleton, D. M. *J. Am. Chem. Soc.* **2010**, *132*, 15130–15132. (d) Ribeiro-Viana, R.; Sánchez-Navarro, M.; Luczkowiak, J.; Koeppel, J. R.; Delgado, R.; Rojo, J.; Davis, B. G. *Nat. Commun.* **2012**, *3*, 1303. For a recent review, see: (e) Varner, C. T.; Rosen, T.; Martin, J. T.; Kane, R. S. *Biomacromolecules* **2015**, *16*, 43–55.

(4) (a) Holub, J. M.; Garabedian, M. J.; Kirshenbaum, K. *Mol. BioSyst.* **2011**, *7*, 337–345. (b) Pushechnikov, A.; Lee, M. M.; Childs-Disney, J. L.; Sobczak, K.; French, J. M.; Thornton, C. A.; Disney, M. D. *J. Am. Chem. Soc.* **2009**, *131*, 9767–9779. (c) Levine, P. M.; Imberg, K.; Garabedian, M. J.; Kirshenbaum, K. *J. Am. Chem. Soc.* **2012**, *134*, 6912–6915.

(5) Yu, S.; Dong, R.; Chen, J.; Chen, F.; Jiang, W.; Zhou, Y.; Zhu, X.; Yan, D. *Biomacromolecules* **2014**, *15*, 1828–1836. (b) Zhang, Z.; Ali, M. M.; Eckert, M. A.; Kang, D.-K.; Chen, Y. Y.; Sender, L. S.; Fruman, D. A.; Zhao, W. *Biomaterials* **2013**, *34*, 9728–9735. (c) Wang, J.; Tian, S.; Petros, R. A.; Napier, M. E.; DeSimone, J. M. *J. Am. Chem. Soc.* **2010**, *132*, 11306–11313. (d) Pokorski, J. K.; Hovlid, M. L.; Finn, M. G. *ChemBioChem* **2011**, *12*, 2441–2447. (e) Shuvaev, V. V.; Iliès, M. A.; Simone, E.; Zaitsev, S.; Kim, Y.; Cai, S.; Mahmud, A.; Dziubla, T.; Muro, S.; Discher, D. E.; Muzykantov, V. R. *ACS Nano* **2011**, *5*, 6991–6999.

(6) Sahay, G.; Alakhova, D. Y.; Kabanov, A. V. *J. Controlled Release* **2010**, *145*, 182–195.

(7) For selected recent reviews see: (a) Bernat, V.; Disney, M. D. *Neuron* **2015**, *87*, 28–46. (b) Chang, C.-K.; Jhan, C.-R.; Hou, M.-H. *Curr. Top. Med. Chem.* **2015**, *15*, 1398–1408. (c) Usdin, K.; House, N. C.; Freudenreich, C. H. *Crit. Rev. Biochem. Mol. Biol.* **2015**, *50*, 142–167. (d) Mohan, A.; Goodwin, M.; Swanson, M. S. *Brain Res.* **2014**, *1584*, 3–14. (e) Duan, R. H.; Sharma, S.; Xia, Q. P.; Garber, K.; Jin, P. *J. Genet. Genomics* **2014**, *41*, 473–484. (f) Kiliszek, A.; Rypniewski, W. *Nucleic Acids Res.* **2014**, *42*, 8189–8199. (g) Sicot, G.; Gomes-Pereira, M. *Biochim. Biophys. Acta, Mol. Basis Dis.* **2013**, *1832*, 1390–1409.

(8) (a) Ranum, L. P. W.; Cooper, T. A. *Annu. Rev. Neurosci.* **2006**, *29*, 259–277. (b) Wheeler, T. M.; Thornton, C. A. *Curr. Opin. Neurol.* **2007**, *20*, 572–576. (c) Orr, H. T.; Zoghbi, H. Y. *Annu. Rev. Neurosci.* **2007**, *30*, 575–621.

(9) (a) Gareiss, P. C.; Sobczak, K.; McNaughton, B. R.; Palde, P. B.; Thornton, C. A.; Miller, B. L. *J. Am. Chem. Soc.* **2008**, *130*, 16254–16261. (b) Wheeler, T. M.; Sobczak, K.; Lueck, J. D.; Osborne, R. J.; Lin, X.; Dirksen, R. T.; Thornton, C. A. *Science* **2009**, *325*, 336–339. (c) Arambula, J. F.; Ramisetty, S. R.; Baranger, A. M.; Zimmerman, S. C. *Proc. Natl. Acad. Sci. U. S. A.* **2009**, *106*, 16068–16073. (d) Warf, M. B.; Nakamori, M.; Matthys, C. M.; Thornton, C. A.; Berglund, J. A. *Proc. Natl. Acad. Sci. U. S. A.* **2009**, *106*, 18551–18556. (e) García-López, A.; Llamusi, B.; Orzáez, M.; Pérez-Payá, E.; Artero, R. D. *Proc. Natl. Acad. Sci. U. S. A.* **2011**, *108*, 11866–11871. (f) Parkesh, R.; Childs-Disney, J. L.; Nakamori, M.; Kumar, A.; Wang, E.; Wang, T.; Hoskins, J.; Tran, T.; Housman, D.; Thornton, C. A.; Disney, M. D. *J. Am. Chem. Soc.* **2012**, *134*, 4731–4742. (g) Wong, C.-H.; Nguyen, L.; Peh, J.; Luu, L. M.; Sanchez, J. S.; Richardson, S. L.; Tuccinardi, T.; Tsoi, H.; Chan, W. Y.; Chan, H. Y. E.; Baranger, A. M.; Hergenrother, P. J.; Zimmerman, S. C. *J. Am. Chem. Soc.* **2014**, *136*, 6355–6361. (h) Nguyen, L.; Luu, L. M.; Peng, S.; Serrano, J. F.; Chan, H. Y. E.; Zimmerman, S. C. *J. Am. Chem. Soc.* **2015**, *137*, 14180–14189.

(10) (a) Lee, M. M.; Pushechnikov, A.; Disney, M. D. *ACS Chem. Biol.* **2009**, *4*, 345–355. (b) Childs-Disney, J. L.; Parkesh, R.;

- Nakamori, M.; Thornton, C. A.; Disney, M. D. *ACS Chem. Biol.* **2012**, *7*, 1984–1993. (c) Jahromi, A. H.; Fu, Y.; Miller, K. A.; Nguyen, L.; Luu, L. M.; Baranger, A. M.; Zimmerman, S. C. *J. Med. Chem.* **2013**, *56*, 9471–9481. (d) Jahromi, A. H.; Honda, M.; Zimmerman, S. C.; Spies, M. *Nucleic Acids Res.* **2013**, *41*, 6687–6697.
- (11) For selected reviews of CPPs and CPP mimics, see: (a) Nakase, I.; Kawaguchi, Y.; Nomizu, M.; Futaki, S. *Trends Glycosci. Glycotechnol.* **2015**, *27*, 81–88. (b) deRonde, B. M.; Tew, G. N. *Biopolymers* **2015**, *104*, 265–280. (c) Copolovici, D. M.; Langel, K.; Eriste, E.; Langel, Ü. *ACS Nano* **2014**, *8*, 1972–1994. (d) Stanzl, E. G.; Trantow, B. M.; Vargas, J. R.; Wender, P. A. *Acc. Chem. Res.* **2013**, *46*, 2944–2954. (e) Matile, S.; Vargas Jentsch, A.; Montenegro, J.; Fin, A. *Chem. Soc. Rev.* **2011**, *40*, 2453–2474. For selected examples see: (f) Hennig, A.; Gabriel, G. J.; Tew, G. N.; Matile, S. *J. Am. Chem. Soc.* **2008**, *130*, 10338–10344. (g) Gasparini, G.; Bang, E.-K.; Molinar, G.; Tulumello, D. V.; Ward, S.; Kelley, S. O.; Roux, A.; Sakai, N.; Matile, S. *J. Am. Chem. Soc.* **2014**, *136*, 6069–6074. (h) Daniels, D. S.; Schepartz, A. *J. Am. Chem. Soc.* **2007**, *129*, 14578–14579. (i) Smith, B. A.; Daniels, D. S.; Coplin, A. E.; Jordan, G. E.; McGregor, L. M.; Schepartz, A. *J. Am. Chem. Soc.* **2008**, *130*, 2948–2949. (j) Weinstein, R.; Savariar, E. N.; Felsen, C. N.; Tsien, R. Y. *J. Am. Chem. Soc.* **2014**, *136*, 874–877. (k) Olson, E. S.; Jiang, T.; Aguilera, T. A.; Nguyen, Q. T.; Ellies, L. G.; Scadeng, M.; Tsien, R. Y. *Proc. Natl. Acad. Sci. U. S. A.* **2010**, *107*, 4311–4316. (l) Futaki, S.; Suzuki, T.; Ohashi, W.; Yagami, T.; Tanaka, S.; Ueda, K.; Sugiura, Y. *J. Biol. Chem.* **2001**, *276*, 5836–5840.
- (12) (a) Gabrielson, N. P.; Lu, H.; Yin, L. C.; Li, D.; Wang, F.; Cheng, J. *J. Angew. Chem., Int. Ed.* **2012**, *51*, 1143–1147. (b) Tang, H.; Yin, L.; Kim, K. H.; Cheng, J. *Chem. Sci.* **2013**, *4*, 3839–3844. (c) Zhang, R.; Song, Z.; Yin, L.; Zheng, N.; Tang, H.; Lu, H.; Gabrielson, N. P.; Lin, Y.; Kim, K.; Cheng, J. *WIREs Nanomed. Nanobiotechnol.* **2015**, *7*, 98–110.
- (13) (a) Kolb, H. C.; Finn, M. G.; Sharpless, K. B. *Angew. Chem., Int. Ed.* **2001**, *40*, 2004–2021. (b) Moses, J. E.; Moorhouse, A. D. *Chem. Soc. Rev.* **2007**, *36*, 1249–1262.
- (14) Tang, H.; Zhang, D. *Biomacromolecules* **2010**, *11*, 1585–1592.
- (15) Tang, H.; Li, Y.; Lahasky, S. H.; Sheiko, S. S.; Zhang, D. *Macromolecules* **2011**, *44*, 1491–1499.
- (16) Lu, H.; Cheng, J. *J. Am. Chem. Soc.* **2007**, *129*, 14114–14115.
- (17) Engler, A. C.; Lee, H.-i.; Hammond, P. T. *Angew. Chem., Int. Ed.* **2009**, *48*, 9334–9338.
- (18) Verdonck, B.; Gohy, J.-F.; Khoussakoun, E.; Jérôme, R.; Du Prez, F. *Polymer* **2005**, *46*, 9899–9907.
- (19) Bai, Y.; Lu, H.; Ponnusamy, E.; Cheng, J. *Chem. Commun.* **2011**, *47*, 10830–10832.
- (20) Mansbach, R. A.; Ferguson, A. L. *J. Chem. Phys.* **2015**, *142*, 105101.
- (21) Xiong, M.; Lee, M. W.; Mansbach, R. A.; Song, Z.; Bao, Y.; Peek, R. M.; Yao, C.; Chen, L. F.; Ferguson, A. L.; Wong, G. C.; Cheng, J. *Proc. Natl. Acad. Sci. U. S. A.* **2015**, *112*, 13155–13160.
- (22) Jahromi, A. H.; Nguyen, L.; Fu, Y.; Miller, K. A.; Baranger, A. M.; Zimmerman, S. C. *ACS Chem. Biol.* **2013**, *8*, 1037–1043.
- (23) Gradinaru, C. C.; Marushchak, D. O.; Samim, M.; Krull, U. J. *Analyst* **2010**, *135*, 452–459.
- (24) Gestwicki, J. E.; Cairo, C. W.; Strong, L. E.; Oetjen, K. A.; Kiessling, L. L. *J. Am. Chem. Soc.* **2002**, *124*, 14922–14933.
- (25) Boisguérin, P.; Deshayes, S.; Gait, M. J.; O'Donovan, L.; Godfrey, C.; Betts, C. A.; Wood, M. J. A.; Lebleu, B. *Adv. Drug Delivery Rev.* **2015**, *87*, 52–67.
- (26) (a) Taneja, K. L.; McCurrach, M.; Schalling, M.; Housman, D.; Singer, R. H. *J. Cell Biol.* **1995**, *128*, 995–1002. (b) Davis, B. M.; McCurrach, M. E.; Taneja, K. L.; Singer, R. H.; Housman, D. E. *Proc. Natl. Acad. Sci. U. S. A.* **1997**, *94*, 7388–7393.
- (27) For examples on the use of GFP-DT960, see: (a) Lee, J. E.; Bennett, C. F.; Cooper, T. A. *Proc. Natl. Acad. Sci. U. S. A.* **2012**, *109*, 4221–4226. (b) Kalsotra, A.; Singh, R. K.; Gurha, P.; Ward, A. J.; Creighton, C. J.; Cooper, T. A. *Cell Rep.* **2014**, *6*, 336–345. (c) Nguyen, L.; Lee, J.; Wong, C.-H.; Zimmerman, S. C. *ChemMedChem* **2014**, *9*, 2455–2462.
- (28) Jog, S. P.; Paul, S.; Dansithong, W.; Tring, S.; Comai, L.; Reddy, S. *PLoS One* **2012**, *7*, e48825.
- (29) Savkur, R. S.; Philips, A. V.; Cooper, T. A. *Nat. Genet.* **2001**, *29*, 40–47.
- (30) King, A.; Chakrabarty, S.; Zhang, W.; Zeng, X.; Ohman, D. E.; Wood, L. F.; Abraham, S.; Rao, R.; Wynne, K. J. *Biomacromolecules* **2014**, *15*, 456–467.
- (31) Pearson, C. E. *PLoS Genet.* **2011**, *7*, e1002018.
- (32) Perbellini, R.; Greco, S.; Sarra-Ferraris, G.; Cardani, R.; Capogrossi, M. C.; Meola, G.; Martelli, F. *Neuromuscular Disord.* **2011**, *21*, 81–88.
- (33) Nguyen, L.; Luu, L. M.; Peng, S.; Serrano, J. F.; Chan, H. Y. E.; Zimmerman, S. C. *J. Am. Chem. Soc.* **2015**, *137*, 14180–14189.
- (34) Tung, C. H.; Wei, Z. P.; Leibowitz, M. J.; Stein, S. *Proc. Natl. Acad. Sci. U. S. A.* **1992**, *89*, 7114–7118.
- (35) Miller, J. W.; Urbinati, C. R.; Teng-umnuay, P.; Stenberg, M. G.; Byrne, B. J.; Thornton, C. A.; Swanson, M. S. *EMBO J.* **2000**, *19*, 4439–4448.
- (36) Garcia-Lopez, A.; Monferrer, L.; Garcia-Alcover, I.; Vicente-Crespo, M.; Alvarez-Abril, M. C.; Artero, R. D. *PLoS One* **2008**, *3*, e1595.
- (37) Lanson, N. A.; Maltare, A.; King, H.; Smith, R.; Kim, J. H.; Taylor, J. P.; Lloyd, T. E.; Pandey, U. B. *Hum. Mol. Genet.* **2011**, *20*, 2510–2523.